A Thermal Habitat for RNA Amplification and Accumulation

Annalena Salditt[a#], Lorenz M. R. Keil[a#], David P. Horning[b#], Christof B. Mast[a], Gerald F. Joyce[b] & Dieter Braun[a*]

Affiliations: [a]Systems Biophysics, Physics Department, Center for Nanoscience, Ludwig-Maximilians-Universität München, 80799 Munich, Germany

[b]The Salk Institute, 10010 N. Torrey Pines Road, La Jolla, CA 92037

* Corresponding author. Email: dieter.braun@lmu.de; Phone: +49-89-2180-1484

# Contributed equally

The RNA world scenario posits replication by RNA polymerases. On early Earth, a geophysical setting is required to separate hybridized strands after their replication and to localize them against diffusion. We present a pointed heat source that drives exponential, RNA-catalyzed amplification of short RNA with high efficiency in a confined chamber. While shorter strands were periodically melted by laminar convection, the temperature gradient caused aggregated polymerase molecules to accumulate, protecting them from degradation in hot regions of the chamber. These findings demonstrate a size-selective pathway for autonomous RNA-based replication in a natural non-equilibrium condition.

Introduction

In modern living systems, the translation of information from DNA to proteins is performed by an RNA intermediate, separating the requirements for the replication of genetic polymers and the production of functional enzymes. However, RNA itself is capable of both, storing genetic information and folding into catalytically active structures, including those that enable copying of RNA molecules[1–3]. Thus, a solution for storage and effective transfer of information on early Earth prior to the invention of genetically-encoded proteins could have been achieved with an RNA-only replication mechanism[4–8].

Any RNA copying mechanism, based on either templated ligation or templated polymerization, relies on Watson-Crick base pairing. An energy source is needed to separate the two complementary strands to begin the next round of templated synthesis, which would need to have been provided by a plausible geochemical mechanism on the early Earth. Separation of hybridized strands could be achieved by pH cycling[9,10], evaporation-wetting cycles[11–13], oscillation of salt concentrations[14], or elevated temperatures. In all cases, a setting is needed that minimizes the spontaneous cleavage of RNA[15,16] that occurs at high temperatures for the high-salt conditions required for RNA catalysis. In the temperature range from 20 °C to 90 °C, degradation increases over 4 orders of magnitude, dictating a minimal exposure time at high temperatures.

A habitat for RNA replication on the early Earth should not only be able to separate double-stranded RNA, but also provide a mechanism for its persistent accumulation against dilution by diffusion. Previous studies have shown that a localized heat flux across closed, elongated compartments can accumulate nucleic acids. This mechanism favors the retention of longer strands in a replication reaction mixture[17,18]. While the combination of replication and selection was shown for the protein-based replication of DNA using Taq DNA polymerase[19], also in combination with accumulation[20,21], it was unclear whether the thermal instability of RNA would prevent a similar approach.

Here, we describe a modified thermal microenvironment that is able to drive the replication of small RNAs catalyzed by a larger polymerase ribozyme. A punctual heat source inside a cylindrical compartment gives rise to two effects: (i) laminar gravitational convection due to the temperature-dependent density of water, resulting in temperature cycles that meet the delicate requirements for the elongation and strand separation for RNA-catalyzed RNA replication; and (ii) thermophoretic

movement of molecules along a temperature gradient, pointing outwards from the high temperature spot (Figure 1a). This thermophoretic movement has been shown to depend on a combination of non-ionic interactions, ionic shielding, and Seebeck effects[22]. In the case of polyanionic nucleic acids at elevated temperatures, thermophoresis drives the molecules from warmer to cooler areas[26]. For a cylindrical compartment, the interplay of convective and thermophoretic transport resulted in a length-dependent net transport of molecules away from the warm temperature spot. The efficiency of this transport increased for longer RNAs, stabilizing them against cleavage that would occur at higher temperatures.

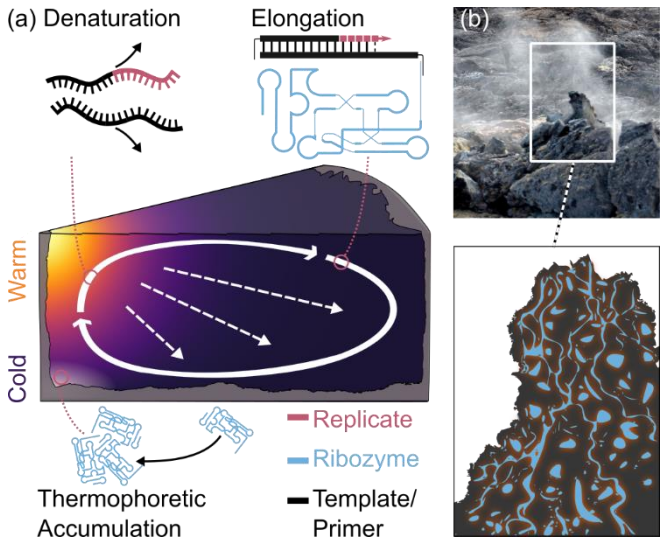

Figure 1. Heat flux across water-filled pores drives RNA-catalyzed RNA replication. (a) A heat flow is used to create a temperature differences across a water filled pore. The temperature differences induce both thermophoresis of molecules (dashed arrows), moving them along thermal gradients, and convection of water (solid arrows). Simulations predict that the interplay of the two physical non-equilibrium effects locally concentrates the RNA polymerase toward cold regions of the cylindrical chamber, where it is protected against thermal degradation. Due to the strong length-dependent thermophoretic properties of RNA[22], shorter RNA molecules are not accumulated, but are subjected to temperature oscillations to achieve the necessary strand separation in the warm spot after their template-directed replication in the cold areas. (b) A natural setting for such a heat flow could be the dissipation of heat across volcanic or hydrothermal rocks. This leads to temperature differences over porous structures of various shapes and lengths.

In contrast, the replicated shorter RNA oligomers cycled quickly through the hotter areas of the habitat, where they could undergo thermally-induced denaturation. This cycling ensured the melting of double-stranded molecules, providing templates for new polymerization reactions. As a result, the replication and preservation of genetic information could be accomplished within a single, thermally driven environment. On the early Earth, similar thermal hatcheries could have driven RNA-based replication in natural conditions, provided confinement and temperature gradients(Figure 1b), which are a common setting in volcanic or hydrothermal environments.

Results

Convective temperature oscillations. The heat flow was implemented via a focused infrared laser that was absorbed in a water-filled cylindrical chamber. The resulting radial symmetric temperature profile consisted of a hot temperature spot (~80 °C), decreasing across the compartment to 17 °C at the bottom side, as measured by fluorescent thermometry (see Materials and Methods, SI Figure 1). The emerging temperature gradient not only accounted for the accumulation, but also for the repetitive temperature cycling of the oligonucleotides.

A similar geometry driving protein-catalyzed replication has previously been reported based on localized heating of the chamber surface[23]. Both implementations showed comparable temperature fields in numerical simulations (SI Figure 2). However, protein-catalyzed replication mimics only later stages of evolution, after the emergence of genetically encoded proteins. Here, the amplification of sequence information relied solely on the enzymatic activity of an RNA molecule.

The convection chamber drove RNA-catalyzed amplification of a 35-nucleotide RNA template, employing 25-nucleotide short RNA primers. The slow polymerization rate of the ribozyme required the convection to run for ~24 h. Under these conditions, the convection chamber showed exponential amplification of the 35-nucleotide RNA, with starting template concentrations as low as 100 fM (Figure 2a, b). Thermal cycling of a bulk reaction mixture under optimized conditions achieved similar results with 50 temperature cycles and a cycle time of 20 min. Starting with 100 fM RNA template, RNA-catalyzed amplification resulted in product yields of 2×10^5-fold and 4×10^5-fold for the bulk and convectively driven reactions, respectively (Figure 2d). This amplification could be described theoretically by a two-parameter growth equation (see

Supplementary Information), deriving a similar maximum replication efficiency E, for convection with E = 1.27 and for thermal cycling with E = 1.28. In both cases, the buffer conditions were optimized to increase replication yield[3], *i.e.* by adding PEG8000 to serve as a molecular crowding agent, reducing the concentration of Mg^{2+} to 50 mM to reduce spontaneous cleavage of RNA, and adding tetrapropylammonium chloride (TPA) to lower the melting temperature of the RNA.

To gain access to the temperature cycling conditions within the chamber, a fluorescence measurement of the temperature profile was used as the basis for a numerical model. The temperature cycling of the molecules inside the chamber was based on a combination of laminar convection, Brownian motion, and thermophoretic drift (SI Figure 3). With a chamber thickness of 500 µm, we obtained a mean cycle time of 26 min for the 35-nucleotide RNA to oscillate between the threshold temperatures of 20 and 60 °C (Figure 2 c, d). This matched the 20 min cycling protocol in the thermal cycler (68 °C for 2 s, then 17 °C for 20 min) used in the bulk amplification protocols in the homogeneously mixed experiments[3]. In this way, the molecules evade the fast degradation at high temperatures[24] shown in Figure 2e.

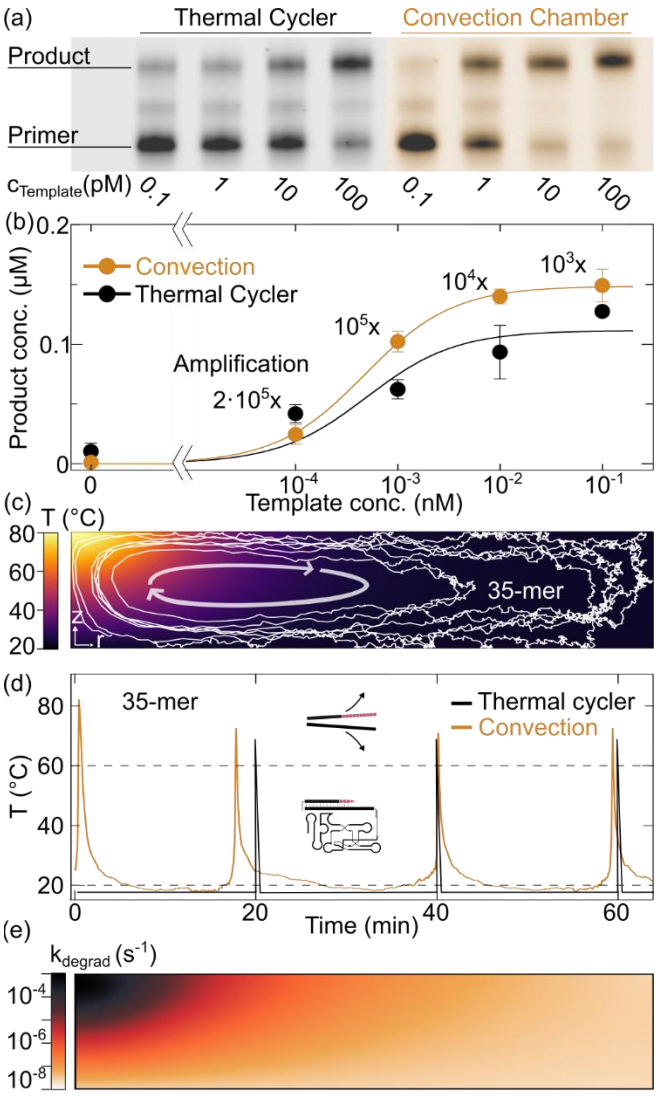

126 **Figure 2. Convective RNA-catalyzed replication of RNA.** (a) The convection system and a thermal
127 cycler showed similar yields of primer extension on the 35-nucleotide RNA template. (b) The polymerase
128 ribozyme exponentially amplified starting template concentrations as low as 100 fM in 24 h. The
129 amplification can be described theoretically by a two-parameter growth equation (Supplementary
130 Information). A maximum amplification of 2×10^5-fold was observed in the convection chamber. Error bars
131 indicate the deviation from duplicate experiments. (c) Thin lines show simulated stochastic trajectories for
132 a 35mer inside the convection chamber of 500 μm height and 2.25 mm radius. (d) In the convection
133 chamber, RNA mostly resided at low-temperature regions, where polymerization could occur, and passed
134 quickly through high-temperature regions that enabled strand separation. Stochastic simulations found a
135 mean temperature cycling time of 26 min. Thermal cycler experiments were performed with cycles of 17 °C
136 for 20 min, then 68 °C for 2 s. (e) Degradation of RNA is almost 4 orders of magnitude faster at higher
137 temperatures[24].

Thermophoretic accumulation of RNA polymerase. We characterized the accumulation behavior of the different RNA components of the system by monitoring fluorescently labeled single- and double-stranded DNA substitutes containing 35 and 210 nucleotides, in addition to the RNA polymerase itself and its DNA analog. The thermophoretic properties of diluted DNA and RNA, either single- or double-stranded, have been shown to be very similar[25]. However, the thermophoretic drift was found to be strongly length dependent[26].

As expected, we found that the shorter DNA barely accumulated in the convection system. Fully double-stranded 210mer DNA showed a central 5-fold accumulation after 60 min at the bottom of the chamber (Figure 3a). These findings are in agreement with finite-element simulations that took into account convection, diffusion, and thermophoresis (Figure 3c).

Interestingly, the active RNA polymerase showed a different, ring-shaped accumulation pattern in colder regions of the chamber. To understand this effect, we performed accumulation experiments for the RNA polymerase, as well as for a DNA analog of the polymerase ribozyme. The RNA polymerase or its DNA analog forms a ternary complex with RNA primer and template via complementary sequences at the 5´ ends of both polymerase and template[3], enabling the molecules to be stained with a fluorescently labeled primer. Imaging the solution with higher resolution in a 40 µm thin capillary revealed that a majority of the RNA polymerase and its DNA analog were present in form of conglomerates at T = 17 °C (Figure 3b).

By individually removing buffer components, the 6 % w/v PEG8000 was found to be the crucial component that induced aggregation (SI Figure 4), both for the RNA and DNA version of the polymerase sequence. Additionally, the conglomerates exhibited a temperature dependence, where heating the solution led to melting of the conglomerates (see SI and movie). For the 35mer single-stranded DNA and 210mer double-stranded DNA, no aggregates were found, as imaging the solution showed homogeneous fluorescence (Figure 3a, top).

For the conglomerates, we could predict with finite element simulations the ring-shaped accumulation region at the top of the chamber after we included the thermophoretic accumulation of PEG and its diffusiophoretic effect on DNA/RNA as reported by Madea *et al.*[27] (SI Figure 3c). For the conglomerates, diffusiophoresis dominated the movement in the temperature gradient, now pointing towards the heating source. However, this inverted force only has an effect near the

boundary walls where flow velocity does not dominate over the slower diffusion of the conglomerates. As a result, the conglomerated RNA or DNA accumulated into a ring, away from the hot temperature spot at the top chamber wall (SI Figure 5).

The diffusiophoretic interaction between PEG and RNA made the accumulation dependent on the binding details of the molecules. Unsaturated, single-stranded molecules could engage in intermolecular interactions and therefore form conglomerates. This behavior is supported by the stark difference between double-stranded DNA and the single-stranded DNA analog of the polymerase sequence.

Simulating the trajectories of 400 particles with random starting positions gave access to the temperature distribution and cycling times for polymerases, double-stranded DNA, and single-stranded DNA, respectively (SI Figure 6). These simulations showed that the ring-shaped accumulation maintained the conglomerates at a temperature of 45 °C and efficiently restricted them to temperatures below 60 °C. Although molecules not forming conglomerates have a higher residence probability at the lowest temperatures, they are frequently subjected to temperatures above 60 °C. Based on the experiments of Li and Breaker[24] the RNA cleavage rate can be predicted for varying temperature, pH and ions (see SI methods), ranging between $2.1 \cdot 10^{-8}$ s^{-1} for 17 °C and $1.2 \cdot 10^{-3}$ s^{-1} for 85 °C. To investigate whether the accumulation indeed protects the ribozyme, we included the cleavage rate in our simulation. The total ribozyme concentration decreased exponentially (SI Figure 7) with a 5-fold reduced degradation rate if the phoretic forces were activated in the simulation and therefore accumulated the ribozyme conglomerates in the ring pattern. The degradation is predicted to occur over days which make experimental tests difficult. These simulation capabilities will allow us to engineer optimal rock geometries, a process that would have been performed by natural selection on early Earth.

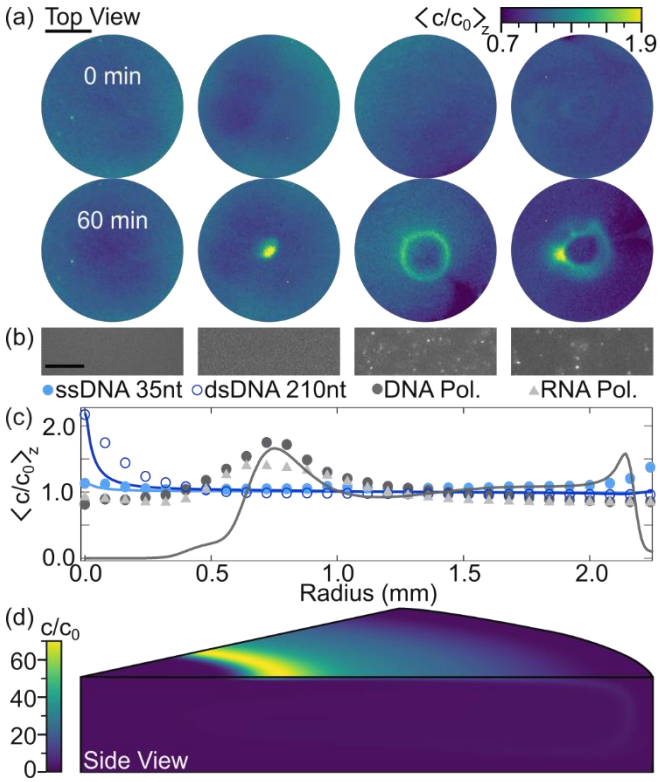

Figure 3. Thermophoretic accumulation of nucleic acids. (a) Accumulation of nucleic acids inside the convection chamber with a central heat source implemented via an IR-laser for 35mer single-stranded DNA, 210mer double-stranded DNA, and folded single-stranded DNA and RNA corresponding to the polymerase sequences (from left to right). The scale bar corresponds to 1 mm. (b) Imaging the different strands inside the reaction buffer revealed the formation of conglomerates in the case of the polymerase sequences. The scale bar corresponds to 250 µm (c) The height average $\langle c/c_0 \rangle_z$ of the simulated relative concentrations (lines) reproduced the experimental fluorescence signal (symbols) for all species. The data points represent the radial averaging of the background corrected fluorescence images with respect to the central point of the chamber. (d) By including diffusive, convective, thermophoretic, and diffusiophoretic transport in the finite element simulation, the model could capture the ring-shaped concentration enhancement of the polymerases observed in the experiments, with a maximum of 66-fold concentration increase after 60 min. The simulation was executed in a compartment of 500 µm and 2.25 mm height and radius, respectively.

191

Discussion

What habitat could provide conditions for an RNA world implementation of the emergence of life? Considerable efforts have been made to investigate the synthesis of RNA by an RNA polymerase ribozyme[3,28–32], but only very few reactions have been operated in a prebiotically plausible setting.

The spontaneous cleavage of RNA at the elevated temperatures necessary to separate template and product strands limits the formation and preservation of longer nucleic acids. On the early Earth, however, longer RNAs would have been required to provide robust enzymatic activities[33,34]. The thermal habitat described here provides temperature conditions that can drive RNA-catalyzed RNA replication. It achieved comparable replication kinetics to the optimized bulk reaction within a standard thermal cycler. Additionally, the interplay of phoretic forces and convection concentrated the RNA polymerase away from the central heating spot. This length-dependent accumulation mechanism biased towards longer and more structured RNAs also could help to overcome the threat of short parasitic sequences that are generally copied more quickly. In the thermal habitat, shorter RNAs have a higher probability of exposure to elevated temperatures where degradation is enhanced (Figure 3a; SI Figure 5)[16]. Moreover, the localization of the ribozymes will be able to feed the reaction with nucleotides with a simple flow through the chamber. The conditions present in the compartment can be tuned to match multiple reaction conditions, which allows us to adapt to future versions of early replication scenarios as well as other reactions.

One such example is the RNA-catalyzed polymerization of RNA, carried out in eutectic ice, which both concentrates the reactants and reduces spontaneous RNA cleavage[32]. Moving forward, including ice phases in future versions of the shown thermal habitant could help to reduce the bulk salt concentrations, while still achieving thermal strand separation and long term localization by thermal convection and thermophoresis.

The experiments indicate the existence of selective pathways in thermal habitats, which could guide RNA evolution towards longer and more structured sequences. This setting could provide a way to replicate not only 35mers, but a complete RNA polymerase that is assembled from several

shorter component strands[31,32,35]. How such >200-nucleotide RNAs could have emerged starting from simple, non-enzymatic replication chemistries in a similar setting remains an open question.

Conclusion

The search for the origin of life implies finding a location for informational molecules to replicate and undergo Darwinian evolution against entropic obstacles such as dilution and spontaneous degradation. The experiments described here demonstrate how a heat flow across a millimeter-sized, water-filled porous rock can lead to spatial separation of molecular species resulting in different reaction conditions for different species. The conditions inside such a compartment can be tuned according to the requirements of the partaking molecules due to the scalable nature of this setting. A similar setting could have driven both the accumulation and RNA-based replication in the emergence of life, relying only on thermal energy, a plausible geological energy source on the early Earth. Current forms of RNA polymerase ribozymes can only replicate very short RNA strands. However, the observed thermal selection bias towards long RNA strands in this system could guide molecular evolution towards longer strands and higher complexity.

Materials and Methods

RNA-catalyzed replication of RNA. The ribozyme was prepared by *in vitro* transcription of double-stranded DNA (20 µg/mL) as described by Horning *et al.*[3]. All RNA oligomers (polymerase, primers, and template) were purified by denaturing polyacrylamide gel electrophoresis (PAGE) and subsequent ethanol precipitation. They were annealed in 10 mM Tris (pH 8), 1 mM EDTA and 0.05 % by heating to 95 °C for 30 s and ramping down to 4 °C at 0.2 °C/s. Annealed RNA was mixed with reaction buffer and NTPs to achieve a final reaction mixture of 400 nM of 24-3 polymerase ribozyme, 200 nM primer, 4 mM NTPs and varying amounts of template, with 50 mM Tris (pH 8.3), 50 mM $MgCl_2$, 6% w/v PEG8000, 0.9 M TPA, and 0.05 % Tween20. The primers were 5´- biotinylated and labeled with fluoroscein. The reaction was quenched by adding 0.5x volumes of 500 mM EDTA (pH 8), then the biotinylated primers and extended products were captured using Streptavidin C1 Dynabeads (ThermoFisher Scientific, USA). The captured materials were washed four times with an alkali solution (25 mM NaOH, 0.05 % TWEEN20, 1 mM EDTA), then two times with a mixture of 8 M urea, 1 mM EDTA, 0.05 % TWEEN20, and 10 mM Tris (pH 8.0). For analysis by PAGE, the materials were mixed with 98 % formamide and 10 mM EDTA, heated at 95 °C for 10 min, then separated in a 12.5 % polyacrylamide gel. The products were imaged by CCD photography (Orca 03-G, Hamamatsu, Japan) through a green bandpass filter (520 nm, 10 nm FWHM, Newport, Germany) using a spectrally filtered source (LED 470 nm, filter 470 nm, 10 nm FWHM, Thorlabs, Germany) and high-quality interference filters (bandpass 692±20 nm, OD 6 blocking, Edmund Optics, USA; bandpass 700±35 nm, OD 2 blocking, Newport, USA) using a filtered source (LED 625 nm, filter 630 nm, 10 nm FWHM, Thorlabs, Germany) for fluorescein- and Cy5 labels, respectively. The bulk control experiments were carried out in a thermocycler with enhanced heating/cooling rates (Analytik Jena AG, Germany).

Convection system. The reaction chamber was constructed from 500 µm thermally conductive soft-silicone film, with blanket out-holes of 5 mm diameter (KU-TCS, Aavid Kunze GmbH, Germany). It was closed at the bottom using a silica wafer (Si-Mat-Silicon Materials e.K., Germany) with a thickness of 525±25 µm and a 100 nm SiO_2 coating. The upper enclosure was a 170 µm borosilicate glass coverslip (Carl Roth, Germany). For the generation of a stable

temperature gradient, an IR laser (TLR-30-Y12, IPG Laser GmbH, Germany) and Peltier element (Uwe Electronic Vertriebs GmbH, Germany) were used as heat source and heat sink, respectively. The temperature of the Peltier element was regulated by a PID-controlled feedback loop in conjunction with a water bath (CF41 Kryo-Kompakt-Thermostat, Julabo, Germany). Fluorescent imaging of the accumulated materials was performed using a long working distance 2× objective (Mitutoyo Plan Apo Infinity 2x, 0.055 NA, Mitutoyo Corporation, Japan), equipped with CCD camera (Stingray F-145B, Allied Vision Technologies GmbH, Germany), illuminated with two alternating LEDs (625 nm and 470 nm, Thorlabs, Germany) in combination with a dual-band filter set (fluorescein and Cy5, AHF, Germany). Scanning mirrors (6200-XY, Cambridge Technology, England) were used to sequentially direct the laser onto four sample chambers. The IR laser was coupled into the optical path between the sample and objective by a cold mirror dichroic (transmission 400–700 nm, reflection 633/1940 nm, AHF, Germany). The temperature profile was measured using the fluorescence of 50 µM 2′,7′-bis-(2-carboxyethyl)-5-(and 6)-carboxyfluorescein), diluted in 10 mM Tris (pH 8.0) and calibrated the temperature dependent fluorescence by varying the temperature of the heat bath.

Acknowledgements

This work was supported by the NanoSystems Initiative Munich, the Simons Collaboration on the Origin of Life. Funding was started by the SFB 1032 Nanoagents Project A4 and finished by the CRC 235 Emergence of Life Project P9. We thank Christina Dirscherl, Patrick Kudella, and Alexandra Kühnlein for helpful comments on the manuscript.

Author contributions

L.K., D.P.H., A.S. and C.B.M. performed the experiments. L.K., D.P.H., A.S., C.B.M., G.F.J., and D.B. conceived and designed the experiments, L.K., D.P.H., A.S., C.B.M., G.F.J. and D.B. analyzed the data and wrote the paper.

Competing financial interests

The authors declare no competing financial interests.

1. Joyce, G. F. Toward an alternative biology. *Science (80-.).* **336**, 307–308 (2012).

2. Attwater, J., Wochner, A., Pinheiro, V. B., Coulson, A. & Holliger, P. Ice as a protocellular medium for RNA replication. *Nat. Commun.* **1**, 76 (2010).

3. Horning, D. P. & Joyce, G. F. Amplification of RNA by an RNA polymerase ribozyme. *Proc. Natl. Acad. Sci.* **113**, 9786–9791 (2016).

4. Gilbert, W. The RNA world. *Nature* vol. 319 618 (1986).

5. Leslie E., O. Prebiotic Chemistry and the Origin of the RNA World. *Crit. Rev. Biochem. Mol. Biol.* **39**, 99–123 (2004).

6. Robertson, M. P. & Joyce, G. F. The Origins of the RNA World. *Cold Spring Harb. Perspect. Biol.* **4**, a003608–a003608 (2012).

7. Pressman, A., Blanco, C. & Chen, I. A. The RNA World as a Model System to Study the Origin of Life. *Curr. Biol.* **25**, R953–R963 (2015).

8. Ban, N. The Complete Atomic Structure of the Large Ribosomal Subunit at 2.4 A Resolution. *Science (80-.).* **289**, 905–920 (2000).

9. Mariani, A., Bonfio, C., Johnson, C. M. & Sutherland, J. D. pH-Driven RNA Strand Separation under Prebiotically Plausible Conditions. *Biochemistry* **57**, 6382–6386 (2018).

10. Keil, L. M. R., Möller, F. M., Kieß, M., Kudella, P. W. & Mast, C. B. Proton gradients and pH oscillations emerge from heat flow at the microscale. *Nat. Commun.* **8**, 1897 (2017).

11. Ross, D. & Deamer, D. Dry/Wet Cycling and the Thermodynamics and Kinetics of Prebiotic Polymer Synthesis. *Life* **6**, 28 (2016).

12. Forsythe, J. G. *et al.* Ester-Mediated Amide Bond Formation Driven by Wet-Dry Cycles: A Possible Path to Polypeptides on the Prebiotic Earth. *Angew. Chemie Int. Ed.* **54**, 9871–9875 (2015).

13. Morasch, M. *et al.* Heated gas bubbles enrich, crystallize, dry, phosphorylate and encapsulate prebiotic molecules. *Nat. Chem.* **11**, 779–788 (2019).

14. Ianeselli, A., Mast, C. B. & Braun, D. Periodic Melting of Oligonucleotides by Oscillating Salt Concentrations Triggered by Microscale Water Cycles Inside Heated Rock Pores. *Angewante Chemie* **131**, 13289–13294 (2019).

15. Levy, M. & Miller, S. L. The stability of the RNA bases: Implications for the origin of life. *Proc. Natl. Acad. Sci.* **95**, 7933–7938 (1998).

16. AbouHaidar, M. G. & Ivanov, I. G. Non-Enzymatic RNA Hydrolysis Promoted by the Combined Catalytic Activity of Buffers and Magnesium Ions. *Zeitschrift für Naturforsch. C* **54**, 542–548 (1999).

17. Baaske, P. *et al.* Extreme accumulation of nucleotides in simulated hydrothermal pore systems. *Proc. Natl. Acad. Sci.* **104**, 9346–9351 (2007).

18. Mast, C. B., Schink, S., Gerland, U. & Braun, D. Escalation of polymerization in a thermal gradient. *Proc. Natl. Acad. Sci.* **110**, 8030–8035 (2013).

19. Braun, D., Goddard, N. L. & Libchaber, A. Exponential DNA Replication by Laminar Convection. *Phys. Rev. Lett.* **91**, 158103 (2003).

20. Kreysing, M., Keil, L., Lanzmich, S. & Braun, D. Heat flux across an open pore enables the continuous replication and selection of oligonucleotides towards increasing length. *Nat. Chem.* **7**, 203–208 (2015).

21. Mast, C. B. & Braun, D. Thermal Trap for DNA Replication. *Phys. Rev. Lett.* **104**, 188102 (2010).

22. Reichl, M., Herzog, M., Götz, A. & Braun, D. Why Charged Molecules Move Across a Temperature Gradient: The Role of Electric Fields. *Phys. Rev. Lett.* **112**, 198101 (2014).

23. Hennig, M. & Braun, D. Convective polymerase chain reaction around micro immersion heater. *Appl. Phys. Lett.* **87**, 183901 (2005).

24. Li, Y. & Breaker, R. R. Kinetics of RNA degradation by specific base catalysis of transesterification involving the 2γ-hydroxyl group. *J. Am. Chem. Soc.* **121**, 5364–5372 (1999).

25. Reichl, M., Herzog, M., Greiss, F., Wolff, M. & Braun, D. Understanding the similarity in thermophoresis between single- and double-stranded DNA or RNA. *Phys. Rev. E* **91**, 062709 (2015).

26. Duhr, S. & Braun, D. Why molecules move along a temperature gradient. *Proc. Natl. Acad. Sci.* **103**, 19678–19682 (2006).

27. Maeda, Y. T., Tlusty, T. & Libchaber, A. Effects of long DNA folding and small RNA stem-loop in thermophoresis. *Proc. Natl. Acad. Sci.* **109**, 17972–17977 (2012).

28. Nissen, P., Hansen, J., Ban, N., Moore, P. B. & Steitz, T. A. The structural basis of ribosome activity in peptide bond synthesis. *Science (80-.).* **289**, 920–930 (2000).

29. Ekland, E. H. & Bartel, D. P. RNA-catalysed RNA polymerization using nucleoside trlphosphates. *Lett. to Nat.* **383**, 1996 (1996).

30. Johnston, W. K., Unrau, P. J., Lawrence, M. S., Glasner, M. E. & Bartel, D. P. RNA-catalyzed RNA polymerization: Accurate and general RNA-templated primer extension. *Science (80-.).* **292**, 1319–1325 (2001).

31. Sczepanski, J. T. & Joyce, G. F. A cross-chiral RNA polymerase ribozyme. *Nature* **515**, 440–442 (2014).

32. Mutschler, H., Wochner, A. & Holliger, P. Freeze–thaw cycles as drivers of complex ribozyme assembly. *Nat. Chem.* **7**, 502–508 (2015).

33. Doudna, J., Couture, S. & Szostak, J. A multisubunit ribozyme that is a catalyst of and template for complementary strand RNA synthesis. *Science (80-.).* **251**, 1605–1608 (1991).

34. Adamala, K., Engelhart, A. E. & Szostak, J. W. Generation of Functional RNAs from Inactive Oligonucleotide Complexes by Non-enzymatic Primer Extension. *J. Am. Chem. Soc.* **137**, 483–489 (2015).

35. Attwater, J., Raguram, A., Morgunov, A. S., Gianni, E. & Holliger, P. Ribozyme-catalysed RNA synthesis using triplet building blocks. *Elife* **7**, (2018).